Constructing a Sensitive Control Chart to Monitor Process Mean using Optimal Filter: Time-Frequency Analysis Approach

Maryam Askari[a], Orod Ahmadi[*b], Youness Javid[c]

[a,b,c]Department of Industrial Engineering, Faculty of Engineering, Kharazmi University, Tehran, Iran.

[a]askari_kh_maryam@yahoo.com Tel: +989103004788

[b]orod.ahmadi@khu.ac.ir Tel: +989121231920

[c]Javid@khu.ac.ir Tel: +989124134820

Abstract

Control charts are one of the critical tools for process monitoring. Test statistics are computed as a function of sample means in control charts for monitoring the process mean. In this study, these functions are modeled by filters. These filters have essential properties in both time and frequency domains. In previous studies, only their properties in the time domain have been considered. Thus, the resulting filters have sub-optimal performance. This study investigates the optimal design of these filters for monitoring the process mean. The behavior of these filters is analyzed not only in the time domain but also in the frequency domain. Properties such as stability are considered in designing this filter. An optimization model is designed and solved using a Genetic Algorithm to minimize the Average Run Length. The proposed optimal filter is compared with other control charts using simulation studies. Results showed the high speed of the proposed filter in detecting shifts in the process mean. The proposed optimal filter is also used to monitor the oil price of the OPEC basket. The results showed that shifts were detected at the right time using the proposed optimal filter.

Keywords: Process Monitoring, Control Chart, Signal Processing, Filter Design, Second-order-filter

[*] Corresponding Author: orod.ahmadi@khu.ac.ir

1. Introduction

One of the most important tools of statistical process control is control charts. These charts are used to assess the stability of the processes. It is usually assumed that quality characteristics of interest are well modeled using some univariate or multivariate distributions. Parameters of these distributions must be at nominal levels for the process to be in control. Monitoring univariate distribution is usually performed based on the normality assumption of the quality characteristic of interest with mean, μ and variance, σ^2. In this study, monitoring of the process mean is considered. Different control charts may be used to monitor this parameter. One of the most widely used control charts is the Shewhart $\bar{X}$ control chart. However, the Shewhart control chart usually cannot detect small changes in the process mean.

Some other charts have been proposed in the literature to overcome this problem. The basic idea of these charts is to use some test statistics in which previous samples are taken into account. According to Montgomery [1], two types of these control charts are Cumulative Sum (CUSUM) and Exponentially Weighted Moving Average (EWMA) control charts.

A standard structure may be used to define the test statistics of the control charts mentioned above. In the Shewhart $\bar{X}$ chart, sample means are merely used as test statistics. The CUSUM chart defines the test statistics using the cumulative sum of the sample mean deviations from the in-control mean. Test statistics of the EWMA chart are defined by a weighted average of the previous sample means. In all of these control charts, some appropriate functions of sample means are used to determine the test statistics. These functions which convert sample means to test statistics are systems. A system is a mechanism that alters inputs to obtain some appropriate outputs.

The converting system should be defined so that shifts can be detected rapidly. To define an appropriate control chart, parameters of the converting system that characterize the behavior of test statistics should be chosen optimally. The primary purpose of this research is to design an optimal converting system and introduce a corresponding control chart to rapidly detect shifts in the process mean.

According to Box et al. [2], many systems used in reality are defined as linear systems. If a linear system is used to convert sample means, test statistics are computed as follows:

$$Y_t = \psi_0 \bar{X}_t + \psi_1 \bar{X}_{t-1} + \psi_2 \bar{X}_{t-2} + \ldots;\ t \in \mathbb{Z} \quad (1)$$

in which Y_t is the test statistics computed at time *t*, $\bar{X}_t$ is the sample mean at time *t*, and $\{\psi_j;\ j = 0,1,2,\ldots\}$ are some appropriate real values, called the impulse responses of the system. In Figure 1 block diagram of this system is shown.

Figure 1: Block diagram of a linear system

The system properties are categorized into time and frequency domain properties. In this study, these two domains are considered simultaneously to design an optimal converting system.

Some authors only consider converting systems in the time domain in the literature on statistical process control. Jiang et al. [3] proposed an ARMA control chart to monitor both i.i.d. and autocorrelated processes by passing the input process through an ARMA filter. Jafarian-Namin et al. [4] utilized an ARMA control chart to monitor autocorrelated data.

The EWMA control chart could also be seen as a filter applied to the input signal sequence. Golosnoy et al. [5] suggested using an EWMA control chart for monitoring a linear measurement error model. Mitra et al. [6] designed an AEWMA-type control chart without prior knowledge about the shift magnitude. Tang et al. [7] presented two procedures to optimally design an AEWMA control chart using median run length and expected median run length. To study other types of EWMA control charts, interested readers may refer to Alevizakos et al. [8], Sanusi et al. [9], Noor-ul-Amin [10], and Maravelakis et al. [11].

One other type of control chart that is used to monitor the processes is the CUSUM chart. Hou and Yu [12] developed a log-likelihood-ratio-based CUSUM control chart to monitor arbitrary changes in the probability distribution. Sunthornwat and Areepong [13] derived an explicit formula for the *ARL* of the CUSUM control chart for monitoring seasonal and non-seasonal moving average processes. Rafiei and Asadzadeh [14] proposed a CUSUM control chart to monitor the survival time of patients. Mahamadkhani and Amiri [15] combined the EWMA and CUSUM charts to monitor the process mean effectively. Awais and Haq [16] also proposed Shewhart-EWMA combinations to monitor the process mean.

Control charts are usually designed based on the assumption of data independence over time. According to the increasing rate of automation in processes, data are collected at adjacent times, which are usually correlated. Some authors studied the design of control charts in the time domain for correlated data. Tyagi and Yadav [17] designed a Modified Mixed EWMA and CUSUM (MMEC) control chart to monitor autocorrelated observations. Supharakonsakun [18] studied the performance of a modified EWMA chart for monitoring autocorrelated observations. Khusna et al. [10] proposed a Max-CUSUM control chart for monitoring autocorrelated observations.

Chen and Yu [20] proposed a deep learning approach for monitoring autocorrelated observations. Li et al. [21] used the EWMA control chart to monitor the residual of the p-th order autoregressive model. Keshavarz et al. [22] modified the accelerated failure time regression model to account for the autocorrelated data. Zhou et al [23] designed an attribute control chart to monitor the mean of autocorrelated processes. Li et al. [24] proposed a hidden Markov model to monitor autocorrelated observations.

A system expressed by Equation 1 is usually called a linear filter. The filter parameters are consequential in determining system behavior and should be correctly determined. Principals of filter design were introduced by Oppenheim et al. [25]. Some authors proposed process monitoring based on filtering. He and Hu [26] designed a Chebyshev lowpass filter optimally. Chin and Apley [27] considered the design of a control chart as an optimal linear filter design problem in the time domain. One disadvantage of this method is that computing the output of their linear filter can be somewhat time-consuming to implement.

To overcome this drawback, Chin and Apley [28] proposed a control chart based on a second-order linear filter. However, they only studied the time domain behavior for filter design. Han et al. [29] also proposed a nonlinear filter to construct a control chart.

Some authors used control charts in conjunction with time-frequency analysis. However, they did not design control charts optimally. Teng et al. [30] proposed a data-driven method to monitor a bearing. Jawad and Jaber [31] used the CUSUM control chart to develop a fault detection system for bearings based on time-domain analysis. Teng et al. [32] used the Shewhart control chart to monitor the rotating machine condition based on the time-frequency analysis.

Ahmadi and Shahriari [33], designed filters in the frequency domain to monitor the process mean. However, they did not optimize filters in time and frequency domains.

1-1- Research Gap

Different approaches for designing control charts that are addressed above could be categorized into five main classes shown in Table 1. In all of these approaches, a filter design problem is implicitly studied.

Table 1: Summarized literature review

Table 1 shows that almost all research in the field of statistical process monitoring is limited in the time domain. In these approaches, filters are designed to have suitable properties only in the time domain. However, some properties of filters may not be unfolded in the time domain. As well as time domain properties, filters have some properties in the frequency domain.

A co-occurrence analysis was conducted using the Web of Science database to shed some light on the research gap. In this analysis, 595 articles published from 12/30/1992 to 12/30/2022, which include terms such as Control Chart, ARMA Chart, and Linear Filter were considered. A total number of 87 important author keywords of these articles were assessed for constructing the co-occurrence network. Using R software, these author keywords were processed to determine their co-occurrences. The resulting co-occurrence network, which is the output of Gephi software, is shown in Figure 2.

Figure 2: The co-occurrence network of essential keywords

In Figure 2, author keywords are represented by the network nodes. If two keywords are mentioned in an article simultaneously, an edge is drawn between the nodes corresponding to those two keywords. The width of an edge represents the co-occurrence frequency. As seen in Figure 2, the node “control chart” is only connected to the node “signal processing” with a thin edge. It means that these two keywords were stated simultaneously only one time. As stated earlier, almost all research was conducted to develop control charts considering only the time domain properties of filters. A few studies were conducted to design control charts using the signal and system approach.

Filters' time and frequency properties should be considered simultaneously to construct a control chart properly. Considering only time domain properties of filters may result in control charts with sub-optimal behaviors. Critical features of a filter could be extracted more appropriately using time-frequency analysis.

This paper proposes a unified framework for designing control charts for monitoring the process mean using time-frequency analysis. From Table 1, one may conclude that the time-frequency analysis should be used to design a control chart. This paper studies the essential properties of a second-order filter based on time-frequency analysis. The output of this filter is used to monitor the process. The optimal design of this filter is the primary goal of this research.

The main contributions of this research are as follows:

- Utilizing a converting system to monitor the process mean
- Studying the time domain properties of the converting system
- Studying the frequency domain properties of the converting system
- Optimal design of the converting system using time-frequency analysis
- Constructing a control chart based on the optimal converting system to detect small and moderate shifts as quickly as possible.

The remainder of this paper is organized as follows. In Section 2, some preliminaries about signals and systems are explained. In Section 3, the proposed model for optimal filter design is provided. In Section 4, this model is solved using GA. In Section 5, the performance of the optimal second-order filter is evaluated using simulation studies. A real case study is analyzed and monitored using the proposed optimal filter in Section 6. Finally, results are discussed, and conclusions are made in Section 7.

2. Signal and Systems

It is required to study system properties in time and frequency domains to design an optimal filter. In this research, signals and systems theory is used for system analysis. According to Oppenheim et al. [25], this section provides some preliminaries about signals and systems. A signal is any time-varying function. In this study, discrete in-time signals are considered.

A system is a mechanism that converts an input signal to an output signal. Let $x_t, y_t;\ t \in \mathbb{Z}$ denote the input and output signals of a system, respectively. One class of systems frequently used in practical situations is the Linear Time-Invariant (LTI) system. Input-output relation of this system is as follows:

$$y_t = \psi_0 x_t + \psi_1 x_{t-1} + \psi_2 x_{t-2} + \ldots = \sum_{j=-\infty}^{\infty} \psi_j x_{t-j};\ t \in \mathbb{Z} \tag{2}$$

where $\psi_t = 0;\ t < 0$. As well as expressing a system's input-output relation in the time domain, one may represent this relation in the frequency domain using Discrete-Time Fourier Transformation (DTFT). The DTFT of a signal is defined as:

$$X(e^{i\omega}) = \sum_{t=-\infty}^{\infty} x_t e^{-i\omega t} \tag{3}$$

where $i = \sqrt{-1}$ and ω is called the frequency component. A signal must be absolutely summable, i.e. $\sum_{t=-\infty}^{\infty} |x_t| < \infty$ to have a DTFT. If x_t and ψ_t are both absolutely summable, then one can take DTFT from both sides of Equation 2 and express the input-output relation of a system in the frequency domain as follows:

$$Y(e^{i\omega}) = \Psi(e^{i\omega}) X(e^{i\omega}) \tag{4}$$

in which $Y(e^{i\omega})$ and $\Psi(e^{i\omega})$ are DTFT of y_t and ψ_t, respectively. The function $\Psi(e^{i\omega})$ is usually called the frequency response of a system. The modulus of this function is shown by $|\Psi(e^{i\omega})|$. Filters are systems used to alter the frequency properties of the input signals. Some filters are designed so that $|\Psi(e^{i\omega})|$ vanishes for large values of ω, called lowpass filters. These filters preserve the low frequencies of the input signal, while high frequencies are disappeared in the output. Thus, the input noises are reduced, and a smoother output signal is produced. In Figure 3, the typical shape of $|\Psi(e^{i\omega})|$ for an ideal lowpass filter is shown.

Figure 3: Modulus of frequency response for an ideal lowpass filter

If $\psi_t = 0;\ t < 0$, the filter is called causal. According to this property, the output signal's current value depends on the input signal's current and previous values. For a system to have the frequency response, ψ_t must be absolutely summable. A System with this property is called a stable system.

According to Ogata [34], another property which is required a system to have is the minimum phase property. A minimum phase system reacts to changes in input signal rapidly. Thus, if a sudden shift is introduced in the input signal, this change may be unfolded quickly in the output signal using a minimum phase system.

Not all systems are stable. For non-stable systems, the generalization of DTFT, called Z transformation, may be used to express input-output relations. Let $z = re^{i\omega};\ r > 0$. Then, the Z transform of a signal x_t, is defined as follows:

$$X(z) = \sum_{t=-\infty}^{\infty} x_t z^{-t};\ \ z \in ROC \tag{5}$$

where *ROC* is the Region of Convergence of the Z transform. One may take Z transform from both sides of Equation 1 as follows:

$$Y(z) = \Psi(z)X(z);\ \ z \in ROC \tag{6}$$

in which $Y(z)$ and $\Psi(z)$ are the Z transform of y_t and ψ_t, respectively.

Many linear filters can be shown by a linear difference equation with constant coefficients as follows:

$$\sum_{k=0}^{N-1} a_k y_{t-k} = \sum_{k=0}^{M-1} b_k x_{t-k} \tag{7}$$

where *N* and *M* are some positive integers. Taking the Z transform from both sides of Equation 7, results:

$$\Psi(z) = \frac{Y(z)}{X(z)} = \frac{\sum_{k=0}^{M-1} b_k z^{-k}}{\sum_{k=0}^{N-1} a_k z^{-k}}; \quad z \in ROC \tag{8}$$

The roots of the nominator and denominator of the function shown in Equation 8 are called zeros and poles of the system, respectively. According to Oppenheim [25], all poles must be inside the unit circle for a stable system. For a system to be lowpass, poles must be near +1. In terms of z transformation, a system is said to be causal if its *ROC* lies outside a circle in the z-plane. If all poles and zeros of a system lie inside the unit circle, the system will be the minimum phase.

As an example, suppose that a system has two poles $z_{1,2} = 0.9 \pm 0.1i$. It is also assumed that this system has no zero and the *ROC* of the system is $|z| > 0.91$. In Figure 4 these two poles are shown in the z-plane.

Figure 4: Location of poles for a stable lowpass filter

Since the two poles of this system are inside the unit circle, the corresponding filter is stable. These two poles are near +1. Thus, the filter is also lowpass. According to the location of the system poles, the system is the minimum phase. The *ROC* is the outer region of a circle with the origin as the center. Thus, this system is causal too.

Usually, sample means are used to monitor the process mean. However, the sequence of sample means may be very noisy. Fluctuations in sample means may hide small changes in the process mean. An appropriate filter can remove fluctuations from sample means. This research proposes an optimal second-order filter with some desired properties for monitoring the process mean. In Section 3 design of such a filter is studied.

3. Proposed Model for Optimal Filter Design

All control charts for monitoring the process mean may be seen as filters converting sample means to some test statistics. Many researchers studied the time domain properties of filters and attempted to construct control charts. However, filters have some essential properties in the

frequency domain that should be considered for designing control charts. The main objective of this research is to propose a unified framework for designing the process mean control chart using both time domain and frequency domain properties. This section considers the second-order filter frequency and time domain properties to construct an optimal process mean control chart.

A second-order filter may be represented as follows:

$$y_t = \phi_1 y_{t-1} + \phi_2 y_{t-2} + x_t \; ; \; t \in \mathbb{Z} \tag{9}$$

The filter parameters are shown by $\phi_1 , \phi_2 \in \mathbb{R}$ which must be determined in the filter design procedure. According to Equation 8, the transfer function of this filter is as follows:

$$\Psi(z) = \frac{Y(z)}{X(z)} = \frac{1}{1 - \phi_1 z^{-1} - \phi_2 z^{-2}} = \frac{z^2}{z^2 - \phi_1 z - \phi_2} ; \;\; z \in ROC \tag{10}$$

Different properties of a second-order filter can be expressed using this transfer function.

In designing the proposed optimal second-order filter for monitoring the process mean, some new assumptions are made, listed as follows:

a) The proposed filter should have specific properties in the frequency domain to detect shifts in the process mean as quickly as possible as follows:
   i) Stability
   ii) Lowpass
   iii) Causality
   iv) Minimum phase
b) The proposed filter should also have time domain properties. It is required that the proposed filter detects a predefined critical shift in the process very rapidly.

This paper proposes using a second-order filter to monitor the process mean with properties *a* and *b*, discussed in more detail in the following.

3-1- Stability

The most important property that a second-order filter is required to have is stability. Considering Equation 10, it can be seen that the system has two zeros at $z = 0$. Also, the system has two poles. Solving $z^2 - \phi_1 z - \phi_2 = 0$ for z one can obtain two poles as follows:

$$z_1, z_2 = \frac{\phi_1 \pm \sqrt{\phi_1^2 + 4\phi_2}}{2} \tag{11}$$

According to Oppenheim [25], the filter is stable if the two poles lie inside the unit circle, i.e. $|z_1| < 1$ and $|z_2| < 1$. These conditions are equivalent to the following [2]:

$$\begin{aligned} &-1 < \phi_1 < 1 \\ &\phi_1 + \phi_2 < 1 \\ &\phi_2 - \phi_1 < 1 \end{aligned} \tag{12}$$

3-2- Lowpass

The second-order filter must be lowpass to smooth the input signal. According to Oppenheim [25], the second-order filter is lowpass if $z_1, z_2 \to 1^-$. Therefore, it is proposed in this research that constraints be imposed on the real and imaginary parts of z_1, z_2. Based on these constraints, real and imaginary parts of z_1, z_2 must lie inside a specific interval. In this study, an interval in the vicinity of +0.715 is defined as $(0.715 \pm \delta_1)$ where $\delta_1 = 0.215$. Thus, the real part constraints are defined as follows:

$$\begin{aligned} &0.5 \le \text{Real}(z_1) \le 0.93 \\ &0.5 \le \text{Real}(z_2) \le 0.93 \end{aligned} \tag{13}$$

in which Real(.) is the real part of complex numbers.

As well as real parts, some constraints must be satisfied by imaginary parts of system poles. In this study, an interval is also proposed for imaginary parts of z_1, z_2 as $(0 \pm \delta_2)$ where $\delta_2 = 0.2$. Thus, the imaginary part constraints are proposed as follows:

$$\begin{aligned} &\text{-}0.2 \le \text{Img}(z_1) \le 0.2 \\ &\text{-}0.2 \le \text{Img}(z_2) \le 0.2 \end{aligned} \tag{14}$$

where Img(.) stands for the imaginary part of complex numbers.

3-3- Causality

The output signal of the second-order filter is the test statistics. For these test statistics to be applicable, the current values must be computable based on the input signal's current and previous (not future) values. Thus, the filter should be causal [35]. Considering Equation 9, this filter is causal. No further constraints are needed in this case.

3-4- Minimum Phase

When a shift occurs in the process mean, it is required that the test statistics exceed control limits immediately. Thus, shifts in input signals, e.g., sample means, must be reflected in test statistics with minimum delay. The proposed filter should be the minimum phase to react immediately. The proposed second-order filter has two zeros at $z = 0$ and two poles shown by Equation 11. According to Equation 12, the filter's poles must be chosen inside the unit circle. Thus, by designing a stable filter, all zeros and poles will lie inside the unit circle, and the resulting filter will be the minimum phase.

3-5- Time Domain Constraint

The filter output is plotted on the corresponding control chart. In this study, it is assumed that when the process is in control, the quality characteristic of interest is normally distributed with known mean μ_0 and known variance σ_0^2. If random samples of size *n* are taken from the in-control process, sample means are independently normally distributed with mean μ_0 and variance $\frac{\sigma_0^2}{n}$. In this research, it is proposed to pass the sample means through the second-order filter to reduce noise levels. The proposed test statistics are obtained as follows:

$$Y_t = \phi_1 Y_{t-1} + \phi_2 Y_{t-2} + \bar{X}_t \; ; \; t \in \mathbb{Z} \qquad (15)$$

For the in-control process, Y_t is normally distributed with mean and variance shown in the following [2]:

$$\mu_Y = \frac{\mu_0}{1-\phi_1-\phi_2}$$
$$\sigma_Y^2 = \frac{(1-\phi_2)\sigma_0^2}{n(1+\phi_2)(1-\phi_1-\phi_2)(1+\phi_1-\phi_2)} \quad (16)$$

In this research, the Lower Control Limit (LCL) and Upper Control Limit (UCL) of the proposed control chart are defined as follows:

$$UCL = \mu_Y + L\sigma_Y$$
$$LCL = \mu_Y - L\sigma_Y \quad (17)$$

where $L \geq 0$ is the coefficient of the control chart and must be determined.

In addition to the frequency (z-domain) constraints, a time domain constraint is imposed on the second-order filter and corresponding control chart. The more quickly a control chart detects shifts, the better its performance. The Average Run Length (ARL) is usually used to assess the control charts in the time domain [36]. When the process is in-control, ARL is shown by ARL_0 and for out-of-control conditions, it is shown by ARL_1.

To construct the proposed control chart appropriately, it is assumed that $ARL_0 = 200$. In contrast, ARL_1 needs to be as small as possible for a particular shift in the process mean. This shift is called the critical shift in this study. This study proposes imposing a time domain constraint on the filter as follows:

$$ARL_0(\phi_1, \phi_2, L) = 200 \quad (18)$$

▪

After defining properties that need to be satisfied by the second-order filter, an optimization model is proposed for filter design as follows:

$$\min \; ARL_1(\phi_1, \phi_2, L; \gamma) \quad (19)$$

s.t.

$$-1 < \phi_2 < 1 \quad (20)$$

$$\phi_1 + \phi_2 < 1 \quad (21)$$

$$\phi_2 - \phi_1 < 1 \tag{22}$$

$$0.5 \le \text{Real}\left(\frac{\phi_1 \pm \sqrt{\phi_1^2 + 4\phi_2}}{2} \right) \le 0.93 \tag{23}$$

$$-0.2 \le \text{Img}\left(\frac{\phi_1 \pm \sqrt{\phi_1^2 + 4\phi_2}}{2} \right) \le 0.2 \tag{24}$$

$$ARL_0(\phi_1, \phi_2, L) = 200 \tag{25}$$

$$L \ge 0; \quad \phi_1, \phi_2 \in \mathbb{R} \tag{26}$$

where γ is the critical shift in the process mean. More formally, it is required that when the process's mean changes to a new level, $\mu_0 + \gamma\sigma_0$ the corresponding control chart detects this shift as quickly as possible using a stable, lowpass, causal, and minimum phase filter. The parameters and decision variables of the proposed model are shown in Table 2.

Table 2: Description of model parameters and decision variables

The main objective of the proposed model is to find the values of ϕ_1 , ϕ_2 and *L*, which minimize the out-of-control *ARL* of the proposed control chart for a given value of γ, shown by $ARL_1(\phi_1, \phi_2, L; \gamma)$. It is required that Equation 12 be satisfied by ϕ_1 and ϕ_2 to obtain a stable filter. Thus, these constraints are added to the proposed model, shown by Equations 20, 21, and 22.

Equations 13 and 14 must be satisfied to obtain a second-order lowpass filter. Thus, these two constraints are added to the proposed model and are shown by Equations 23 and 24. According to the structure of the proposed filter, no further constraints are needed to be imposed on the model to obtain a causal and minimum phase filter. The time domain constraint is added to the proposed model, shown in Equation 25. In Section 4, the proposed model is solved using GA for different values of γ.

4. Solving the Proposed Model

It is required to determine the values of filter parameters, ϕ_1, ϕ_2, and L to use the second-order filter. These values may be determined by solving the proposed model. According to the structure of the model objective function and some model constraints, shown in Equations 23, 24, and 25, the proposed model is nonlinear. Note that the complexity of this model is due to the structures of the objective function, $ARL_1(\phi_1, \phi_2, L; \gamma)$, and the time domain constraint, $ARL_0(\phi_1, \phi_2, L) = 200$.

In the proposed method, test statistics are correlated according to Equation 16. The proposed test statistics construct an Autoregressive model of order 2, AR(2). Consequently, *ARL* values cannot be computed using the reciprocal probability of type I or II errors [37]. Thus, methods other than conventional gradient-based optimization are needed to solve this model. However, if *ARL* values are approximated adequately, metaheuristic algorithms may be used to solve this model. Interested readers are referred to Hamidi-Asl et al. [38] and Fasihi et al. [39] for more details about metaheuristic algorithms.

In this study, GA is used to solve the model. Other metaheuristic algorithms, such as the Simulated Annealing (SA) algorithm or Particle Swarm Optimization (PSO), may also be used to solve the model. Interested readers are referred to Abbaszadeh et al. [40] for more details about these algorithms.

In this research, a simulation-based method is used to compute *ARL* values. For given values of ϕ_1, ϕ_2, L, and γ, *ARL* values are approximated using 10000 simulation runs. The proposed procedure to approximate $ARL_0(\phi_1, \phi_2, L)$ is as follows:

Step 0- Let $t = 1$.

Step 1- Generate a random sample of size *n* from the following model:

$$X_{tj} = \mu_0 + \sigma_0 \varepsilon_{tj}; \ \ j = 1, 2, ..., n; \ \ \varepsilon_{tj} \sim N(0,1) \tag{27}$$

Step 2- Based on the sample generated in step 1, compute $\bar{X}_t$. Using the current sample mean and Equation 15, compute test statistics Y_t. The value of μ_Y shown in Equation 16 is used as the initial values of Y_t, i.e., Y_0, Y_{-1}.

Step 3- Compare test statistics Y_t with control limits shown in Equation 17. If $Y_t \in (LCL,UCL)$, $t \leftarrow t+1$ and go to step 1. If $Y_t \notin (LCL,UCL)$, let *RL*=*t* and stop.

This algorithm is repeated 10000 times. The average of *RL*s over 10000 simulation runs is computed. If *RL* in the k^{th} run is shown by RL_k; $k = 1,2,...,10000$, then $A\hat{R}L_0(\phi_1,\phi_2,L) = \frac{1}{10000}\sum_{k=1}^{10000} RL_k$.

To approximate $ARL_1(\phi_1,\phi_2,L;\gamma)$ above algorithm is also used but with a change in step 1. In this step, random samples are generated from the following model:

$$X_{tj} = (\mu_0 + \gamma\sigma_0) + \sigma_0\varepsilon_{tj};\ \ j = 1,2,...,n \tag{28}$$

Using this algorithm to compute *ARL* values, GA can be used to solve the proposed model. In this research, the GA toolbox of MATLAB R2018b is used as an optimization method.

It is required to determine the cost function and constraints of the model for implementing GA. The cost function is shown in Equation 19. Constraints used in GA are shown in Equations 29 to 37.

$$\left|\phi_2\right| - 0.99 \le 0 \tag{29}$$

$$\phi_1 + \phi_2 - 0.99 \le 0 \tag{30}$$

$$\phi_2 - \phi_1 - 0.99 \le 0 \tag{31}$$

$$\text{Real}\left(\frac{\phi_1 \pm \sqrt{\phi_1^2 + 4\phi_2}}{2}\right) - 0.93 \le 0 \tag{32}$$

$$0.5 - \text{Real}\left(\frac{\phi_1 \pm \sqrt{\phi_1^2 + 4\phi_2}}{2}\right) \le 0 \tag{33}$$

$$\text{Img}\left(\frac{\phi_1 \pm \sqrt{\phi_1^2 + 4\phi_2}}{2}\right) - 0.2 \le 0 \tag{34}$$

$$-0.2 - \text{Img}\left(\frac{\phi_1 \pm \sqrt{\phi_1^2 + 4\phi_2}}{2}\right) \le 0 \tag{35}$$

$$\left|ARL_0(\phi_1,\phi_2,L)-200\right|-0.001\le 0 \tag{36}$$

$$L\ge 0;\ \ \phi_1,\phi_2\in\mathbb{R} \tag{37}$$

Equations 29 to 31 are equivalent to Equations 20 to 22. But in formers, the value of 1 is substituted by the value of 0.99, making it possible to use the "$\le$" operator instead of the "$<$" operator. To speed up GA, instead of using Equation 25, an approximation of this equation, shown by Equation 36, is used.

For each solution in GA runs, say $(\phi_{10},\phi_{20},L_0)$, the cost function and constraints need to be computed. The cost function is approximated using the abovementioned algorithm. Note that $ARL_0(\phi_{10},\phi_{20},L_0)$ needs to be computed in Equation 36. In this case, the abovementioned algorithm is also used to approximate this constraint.

In this research, scattered crossover as in [41] and [42], and uniform mutation operators are used in GA. As well as these operators, the probability of crossover (P_c), the probability of mutation (P_m), population size (n_{pop}), and generation number ($iteration$), are determined using the Taguchi design toolbox of MINITAB software. To use the Taguchi design, different levels for GA parameters, shown in Table 3, are considered.

Table 3: Levels of GA parameter used in the Taguchi design

Figure 5 shows the mean values of the signal-to-noise (SN) ratio for different GA parameter levels.

Figure 5: Mean values of SN ratio for different levels of GA parameters

According to the definition of SN ratio, those levels of GA parameters in which the SN ratio is maximal should be selected. Considering Figure 5, it is evident that $iteration=100$, $P_c=0.6$,

$P_m = 0.4$ and $n_{pop} = 100$ should be chosen. Thus, in the following, these values are used to solve the optimization model using GA.

The value of critical shift, γ, must be determined to solve the model. For sensitive processes in which small shifts must be detected, small values for γ should be used. But, for processes in which moderate shifts must be detected rapidly, it should be better to use larger values of γ. In this study, $\gamma = 0.25, 0.5, 1$ are considered. For each value of γ, GA optimizes the proposed model. Optimal values of ϕ_1, ϕ_2 and L are shown in Table 4:

Table 4: Parameters of the optimal second-order filter and the corresponding control chart

The case $\gamma = 0.5$ is considered in more detail to study the behavior of proposed optimal filters. According to Table 4, the input-output relation of this optimal filter is as follows:

$$Y_t = 1.6111 Y_{t-1} - 0.6380 Y_{t-2} + \bar{X}_t \; ; \; t \in \mathbb{Z} \tag{38}$$

According to Equation 10, the transfer function of this filter is expressed by:

$$\Psi(z) = \frac{1}{1 - 1.6111 z^{-1} + 0.638 z^{-2}} ; \; z \in ROC \tag{39}$$

This filter has two zeros at $z = 0$ and two poles at $z_1 = 0.91, z_2 = 0.7011$. These values are shown in Figure 6.

Figure 6: Zeros and poles of the optimal second-order filter for $\gamma = 0.5$

Considering Figure 6, it is evident that both poles of the filter lie inside the unit circle. Thus, the filter shown in Equation 38 is stable. The zeros of this filter are also inside the unit circle. Therefore, this filter is the minimum phase too. This filter is causal, implying that the filter's *ROC* is $|z| > z_1$. Thus, the *ROC* of the filter includes the unit circle $|z| = 1$. Since the filter is

stable, it has a frequency response, $\Psi(e^{i\omega})$. Substituting z by $e^{i\omega}$ in Equation 39, $\Psi(e^{i\omega})$ is obtained as follows:

$$\Psi(e^{i\omega}) = \frac{1}{1-1.6111e^{-i\omega}+0.638e^{-i2\omega}} = \frac{1}{(1-0.91e^{-i\omega})(1-0.7011e^{-i\omega})} \tag{40}$$

In Figure 7, $\left|\Psi(e^{i\omega})\right|$ is depicted over one period, $\omega \in [-\pi, \pi]$.

Figure 7: Modulus of the frequency response of the optimal second-order filter

It can be seen in Figure 7 that $\left|\Psi(e^{i\omega})\right|$ has large values in the vicinity of $\omega = 0$ while it vanishes as $\omega \to \pm\pi$, i.e. for high frequencies. Thus, the intended filter is a lowpass filter.

In Section 5, the performance of the proposed optimal filter and corresponding control chart in detecting shifts in the process mean is evaluated.

5. Performance Evaluation

In this section, the proposed control chart, called AR(2) chart, is compared with other control charts for monitoring the process mean. Comparisons are made via simulation studies by MATLAB R2018b software. Shewhart and EWMA control charts are competitors. Table 5 shows the test statistics and control limits of these charts.

Table 5: Test statistics and control limits of the Shewhart and the EMWA control charts

In Table 5, *L* values for all control charts are determined to have $ARL_0 = 200$.

To compare AR(2) control chart with competitors, *ARL* is used as the first criterion. A control chart with smaller values of out-of-control *ARL* can detect shifts in the process more quickly.

Jaiswal and Kumar [43] stated that the run length distribution is usually right-skewed, especially for small shifts. Thus, as in Qiao et al. [44], more than the *ARL* criterion as a measure of the

performance of control charts is needed. One such performance measure is the Median of Run Length distribution, *MRL*, which is used as the second criterion for performance evaluation.

The third criterion for performance evaluation is the Probability of a False Signal (PFS). This criterion is the percentage of times a control chart warns while the process is in control. The smaller the value of PFS, the better the control chart performance.

For comparison, it is assumed that when the process is in control $\mu_0 = 0$ and $\sigma_0^2 = 1$. Also, for simplicity it is assumed that $n = 1$. To compare the ability of control charts to detect shifts in the process mean, the out-of-control process is modeled as follows:

$$X_t = (\mu_0 + \theta\sigma_0) + \sigma_0\varepsilon_t;\ t = 1,2,...;\ \ \varepsilon_t \sim N(0,1) \qquad (41)$$

where θ is the magnitude of the shift in the process mean. The ability of three control charts to detect various step shifts, $\theta = -2,-1.9,-1.8,...,1.8,1.9,2$, is studied. Parameters of the AR(2) control chart should be determined using the method proposed in Section 4. These parameters are provided in Table 4 for different values of γ.

The Shewhart control chart has one parameter, *L*, which must be determined. For this chart, $L = z_{\alpha/2}$, where $z_{\alpha/2}$ is the upper percentile of standard normal distribution. Using $ARL_0 = 200$, it can be concluded that $L = 2.81$ for the Shewhart control chart.

The EWMA control chart's parameters, λ and L, are determined to detect small shifts quickly while $ARL_0 = 200$. Based on simulation studies, $\lambda = 0.5946$ and $L = 2.8$ were obtained.

Three scenarios for designing the AR(2) control chart were considered. In these scenarios, it is assumed that the critical shift is at low, moderate, and high levels, which can be shown by $\gamma = 0.25, 0.5, 1$, respectively. For each scenario, data were generated from the model shown in Equation 41. *ARL* and *MRL* values were then computed for three control charts based on 10000 simulation runs for different values of θ. Results for the first scenario in which $\gamma = 0.25$ are shown in Figures 8 and 9.

Figure 8: ARL comparison for the first scenario

Figure 9: MRL comparison for the first scenario

Considering Figure 8, it can be seen that when the process is in control, $\theta = 0$, all three control charts have approximately the same *ARL* values. But as $|\theta|$ increases, *ARL* values for the three control charts decrease. However, *ARL* values of the AR(2) chart decrease more rapidly than other control charts. Using the AR(2) control chart, small shifts in the process mean can be detected more rapidly. This phenomenon results from using an optimal lowpass stable filter in AR(2) control chart. High-frequency components in data are removed, and more smooth test statistics are obtained. Small shifts in the process mean are magnified and thus can be detected more quickly.

Figure 9 shows that the *MRL* values for the three control charts decrease as $|\theta|$ increases. For small and moderate shifts in the process, the AR(2) chart's *MRL* values are less than those for the other two control charts. Smaller *MRL* values for the AR(2) chart are also a result of removing high-frequency components from the input signal in the proposed second-order filter.

Results for scenario 2, in which $\gamma = 0.5$, are shown in Figures 10 and 11.

Figure 10: ARL comparison for the second scenario

Figure 11: MRL comparison for the second scenario

Since critical shifts in the first and second scenarios are very similar, the general behavior of the AR(2) control chart in both scenarios is very similar. However, in the second scenario *ARL* curve for the AR(2) vanishes slightly slower than the one in the first scenario.

Results for the third scenario, where $\gamma = 1$, are shown in Figures 12 and 13.

Figure 12: ARL comparison for the third scenario

Figure 13: MRL comparison for the third scenario

Considering Figure 12, one can see that all shifts are detected more rapidly using AR(2) chart. Even for a significant critical shift, the *ARL* curve of the AR(2) control chart damped faster than the Shewhart and EWMA control charts. Considering Figures 8, 10, and 12, it can be seen that the slope of the *ARL* plot for the AR(2) control chart in the third scenario is smaller in absolute value than the ones for the first and second scenarios. Indeed, in the first and second scenarios choosing small values for critical shift results in more sensitive control charts. However, the performance of the proposed AR(2) control chart for the third scenario is acceptable compared to Shewhart and EWMA control charts. According to Figures 9, 11, and 13, the proposed AR(2) control chart performance based on the *MRL* criterion is uniformly superior to the ones for the other two control charts.

The PFS values were also computed for the three abovementioned scenarios. The simulation setting was the same as before. But in each simulation run, it was assumed that the process is in-control for $t = 1,2,...,10$. Samples were generated from the model $X_t = \mu_0 + \sigma_0 \varepsilon_t$, where ε_t s are normally distributed with zero mean and unit variance. For $t = 11,12,...$, the process became out of control, and observations were generated from the model $X_t = (\mu_0 + \theta\sigma_0) + \sigma_0 \varepsilon_t$; $t = 11,12,....$ The PFS was computed in each scenario for different values of θ. Results are shown in Figures 14,15 and 16.

Figure 14: PFS for the first scenario

Figure 15: PFS for the second scenario

Figure 16: PFS for the third scenario

The overall behavior of the three control charts for different values of θ in the three scenarios is the same. The proposed AR(2) control chart has much fewer PFS values in all three scenarios than the other two. This indicates that the proposed control chart generally signals the process is out-of-control after the shift occurs.

The proposed second-order filter is an optimal lowpass filter. According to this property, the proposed optimal filter smooths out the high-frequency components of the input signal. These components are mainly noises. The output signal, plotted on the proposed control chart, becomes smoother by removing noises from the input signal. Thus, the probability of falling test statistics outside the control limits before shifts occur is reduced compared to other sub-optimal control charts.

Simulation results showed that small shifts in the process mean could be detected rapidly and precisely using the proposed optimal lowpass filter. In Section 6, the proposed control chart is used to monitor an actual sequence of observations.

6. Case Study

In this section, an actual data sequence is monitored using the AR(2), Shewhart, and EWMA control charts. The data set is the OPEC basket oil price. Monthly time series data from January 1988 to December 2019, X_t , is studied. This time series is shown in Figure 17.

Figure 17: Time series plot of OPEC basket oil price

Figure 17 shows that some step changes and abrupt jumps occurred in the time series. For financial planning, it is required to find when these changes occurred in the process. One of the main tools for detecting these shifts is a control chart.

A parametric time series model is fitted to the data in the first step. Uncorrelated residuals are then computed using this parametric model. Then, the sequence of residuals is monitored via AR(2), Shewhart, and EWMA control charts.

Figure 18 shows the Sample autocorrelation function (ACF) and sample partial autocorrelation function (PACF) with 95% confidence intervals for the data.

Figure 18: Sample ACF and sample PACF of OPEC basket oil price

From Figure 18, it can be seen that ACF tails off very slowly. This pattern indicates that the time series is non-stationary. This process may be transformed to make it stationary by difference operation. Thus, the first order difference, $X'_t = X_t - X_{t-1}$, was used to remove non-stationarity from the process. Moreover, according to the stability of the first 150 values of X_t, which can be seen in Figure 17, only these 150 values are considered to fit a proper model. Figure 19 illustrates ACF and PACF of the first 150 differenced observations.

Figure 19: Sample ACF and sample PACF of the first 150 differenced observations

Figure 19 shows that the sample ACF of X'_t tails off while its sample PACF cuts off after lag 2. Thus, according to Box et al. [2], a proper ARMA model for the first 150 observations of X'_t is the $AR(2)$ model. Fitting this model to X'_t, the model parameters were estimated as $\hat{\phi}_1^0 = 0.64$, $\hat{\phi}_2^0 = -0.27$, and $\hat{\sigma} = 1.38$, where $\hat{\phi}_1^0$ and $\hat{\phi}_2^0$ are the estimated autoregressive coefficients of X'_t and $\hat{\sigma}$ is the estimated standard deviation of error terms. Based on these parameters, residuals are obtained. X'_t may be expressed as follows:

$$X'_t = 0.64X'_{t-1} - 0.27X'_{t-2} + a_t;\ \ a_t \sim N(0, 1.38^2) \tag{42}$$

The residuals are monitored using AR(2), Shewhart, and EWMA control charts. For constructing AR(2) control chart, filter parameters for $\gamma = 1$ shown in Table 4, were chosen. Shewhart and EWMA control charts' parameters were the same as those explained in Section 5. Control charts are shown in Figure 20.

Figure 20: Control charts of residuals

As shown in Figure 20, fluctuations were removed using the AR(2) chart, and test statistics became more smooth. This chart signals that the process was out of control at $t = 201$. In the Shewhart control chart, residuals were used as test statistics which are very noisy. This high level of noise made test statistics to exceeded the *UCL* earlier. The jump at $t = 31$ was due to random fluctuations, not assignable causes. Thus, the Shewhart control chart wrongly warned of out-of-control conditions at $t = 31$. The EWMA chart also warned of out-of-control conditions at $t = 31$. In summary, the proposed optimal AR(2) chart could smooth out fluctuations and properly detect shifts in the process.

7. Conclusions

In this study, the problem of statistical monitoring of the process mean was considered. Most control charts for monitoring the process mean can be considered as systems that convert sample means to some test statistics. Proper design of these systems can help control charts detect shifts as quickly as possible. The design of such systems was studied in this paper. A second-order-linear filter, was used as a converting system. An optimization model was proposed to design this filter, and the corresponding control chart was constructed. The performance of the proposed control chart was evaluated and compared with Shewhart and EWMA control charts using simulation studies. It was shown that the proposed optimal control chart could detect any step shifts in the process mean rapidly for small, moderate, and large shifts.

Since the proposed second-order filter is a stable and lowpass filter, it removes the high-frequency components in the sequence of sample means. These high-frequency components correspond to noises. The output signal of the proposed second-order filter will be smoother than the input one due to removing noises. Thus, small, moderate, and large shifts in the process mean can be detected more rapidly. The small values of *ARL* and *MRL* show this for the proposed control chart. As a result of the smooth output signal, the probability of false alarms in the corresponding control chart, shown by PFS, would be small too. The proposed optimal control

chart monitored an actual case of OPEC basket oil prices. It was shown that fluctuations were removed from observations and shifts in the process mean could be appropriately detected.

In this paper, the second-order filter was used to obtain test statistics. However, other filters, such as nonlinear and higher-order filters, may also be used to monitor the process mean. In the proposed method, GA was used to solve the optimization model. Other metaheuristic optimization algorithms, including individual-based algorithms, may also be used to speed up solving the filter design problem. The problem of change point detection in the process mean could also be addressed using the proposed second-order filter. The proposed filter was designed to detect critical step shifts. But, the proposed approach could be used to develop an optimal filter to detect other shifts, including sinusoidal, linear trend, spick. These topics may be considered for further research.

References

[1] Montgomery, D.C. "*Introduction to Statistical Quality Control*," 7th edition, John Wiley, New York (2013).

[2] Box, G. E. P., Jenkins, G. M., Reinsel, G. C, et al., "*Time Series Analysis, Forecasting and Control*", 5th edition Prentice-Hall International, New Jersey (2016).

[3] Jiang, W., Tsui, K.L. and Woodall, W.H. "A new SPC monitoring method: The ARMA chart." *Technometrics*, 42(4), pp. 399-410 (2000).

[4] Jafarian-Namin, S., Fallahnezhad, M.S., Tavakkoli-Moghaddam, R., et al., "An integrated quality, maintenance and production model based on the delayed monitoring under the ARMA control chart." *Journal of Statistical Computation and Simulation,* 91(13), pp.2645-2669 (2021).

[5] Golosnoy, V., Hildebrandt, B., Köhler, S., et al., "Control charts for measurement error models." *AStA Advances in Statistical Analysis*, (2022). https://doi.org/10.1007/s10182-022-00462-8.

[6] Mitra, A., Lee, K.B. and Chakraborti, S. "An adaptive exponentially weighted moving average-type control chart to monitor the process mean." *European Journal of Operational Research*, 279(3), pp. 902-911 (2019).

[7] Tang, A., Castagliola, P., Sun, J., et al., "Optimal design of the adaptive EWMA chart for the mean based on median run length and expected median run length." *Quality Technology & Quantitative Management*, 16(4), pp. 439-458 (2019).

[8] Alevizakos, V., Chatterjee, K., and Koukouvinos, C. "The triple exponentially weighted moving average control chart." *Quality Technology & Quantitative Management*, 18(3), pp. 326-354 (2021).

[9] Sanusi, R. A., Teh, S. Y., and Khoo, M. B. "Simultaneous monitoring of magnitude and time-between-events data with a Max-EWMA control chart." *Computers & Industrial Engineering*, 142, 106378 (2020).

[10] Noor-ul-Amin, M. "Impact of measurement error on mixed EWMA-CUSUM control chart." *Scientia Iranica*, (2020).

[11] Maravelakis, P.E., Castagliola, P. and Khoo, M.B. "Run length properties of run rules EWMA chart using integral equations." *Quality Technology & Quantitative Management*, 16(2), pp. 129-139 (2019).

[12] Hou, S., & Yu, K. "A non-parametric CUSUM control chart for process distribution change detection and change type diagnosis." *International Journal of Production Research*, 59(4), pp.1166-1186 (2021).

[13] Sunthornwat, R., & Areepong, Y. "Average run length on CUSUM control chart for seasonal and non-seasonal moving average processes with exogenous variables." *Symmetry*, 12(1), 173 (2020).

[14] Rafiei, N., & Asadzadeh, S. "Designing a risk-adjusted CUSUM control chart based on DEA and NSGA-II approaches (a case study in healthcare: Cardiovascular patients)." *Scientia Iranica* (2020).

[15] Mohamadkhani, A., & Amiri, A. "Developing mixed EWMA-CUSUM and CUSUM-EWMA control charts based on MRSS and DRSS procedures." *Scientia Iranica*, 29(5), pp. 2756-2771 (2022).

[16] Awais, M., and Haq, A. "New Shewhart-EWMA and Shewhart-CUSUM control charts for monitoring process mean." *Scientia Iranica*, 26(6), pp. 3796-3818 (2019).

[17] Tyagi, D., & Yadav, V. "The Modified Mixed Exponentially Weighted Moving Average-Cumulative Sum Control Charts for Autocorrelated Process." *Journal of Reliability and Statistical Studies*, pp.471-490 (2021).

[18] SUPHARAKONSAKUN, Y. “Statistical design for monitoring process mean of a modified EWMA control chart based on autocorrelated data.” *Walailak Journal of Science and Technology (WJST),* 18(12), 19813-12 (2021).

[19] Khusna, H., Mashuri, M., Suhartono, et al., “Residual-based maximum MCUSUM control chart for joint monitoring the mean and variability of multivariate autocorrelated processes.” *Production & Manufacturing Research,* 7(1), pp. 364-394 (2019).

[20] Chen, S., & Yu, J. “Deep recurrent neural network- based residual control chart for autocorrelated processes.” *Quality and Reliability Engineering International,* 35(8), pp. 2687-2708 (2019).

[21] Li, Y., Pan, E. and Xiao, Y. “On autoregressive model selection for the exponentially weighted moving average control chart of residuals in monitoring the mean of autocorrelated processes.” *Quality and Reliability Engineering International*, 36(7), pp. 2351-2369 (2020).

[22] Keshavarz, M., Asadzadeh, S. and Akhavan Niaki, S. "Controlling autocorrelated data in multistage manufacturing processes with an application to textile industry." *Quality and Reliability Engineering International* 35(7) pp. 2314-2326 (2019).

[23] Zhou, W., Cheng, C. and Zheng, Z. “Optimal design of an attribute control chart for monitoring the mean of autocorrelated processes.” *Computer and Industrial Engineering*, 137, p. 106081 (2019).

[24] Li, Y., Li, H., Chen, Z., et al., “An improved hidden Markov model for monitoring the process with autocorrelated observations.” *Energies*, 15(5), p.1685 (2022).

[25] Oppenheim A. V., Wilsky, A. S. and Hamid, S. *Signal and Systems*, Pearson New International Edition (2014).

[26] He, X., and Hu, Z. “Optimization design of fractional- order Chebyshev lowpass filters based on genetic algorithm.” *International Journal of Circuit Theory and Applications.* (2022)

[27] Chin, C.H. and Apley, D.W. “Optimal Design of General Linear Filters for Statistical Process Control.” In *IIE Annual Conference. Proceedings* (p. 1). Institute of Industrial and Systems Engineers (IISE) (2004).

[28] Chin, C.H. and Apley, D.W. “Optimal design of second-order linear filters for control charting.” Technometrics, 48(3), pp. 337-348 (2006).

[29] Han, D., Tsung, F., Li, Y., et al., “A nonlinear filter control chart for detecting dynamic changes.” *Statistica Sinica*, pp. 1077-1096 (2010).

[30] Wang, T., Liu, Z., & Lu, G. “Bearing Condition Monitoring based on the Indicator Generated in Time-frequency Domain.” *In Annual Conference of the PHM Society* (Vol. 11, No. 1), (2019).

[31] Mohammed, J. S., and Abdulhady, J. A. “Rolling bearing fault detection based on vibration signal analysis and cumulative sum control chart.” *FME Transactions*, 49(3), pp. 684-695 (2021).

[32] Wang, T., Lu, G., and Yan, P. “A novel statistical time-frequency analysis for rotating machine condition monitoring.” *IEEE Transactions on Industrial Electronics*, 67(1), 531-541 (2019).

[33] Ahmadi, O. and Shahriari, H. “Monitoring Process Mean Using a Second Order Filter: Signal and System Approach.” *Scientia Iranica*. 29(4), pp. 2210-2229 (2022).

[34] Ogata, K. *Modern control engineering*. Prentice hall (2010).

[35] Gazi, O. *Principals of Signals and Systems*. Springer (2023).

[36] Supharakonsakun, Y., Areepong, Y., & Sukparungsee, S. “The exact solution of the average run length on a modified EWMA control chart for the first-order moving-average process.” *ScienceAsia*, 46(1), pp. 109-118 (2020).

[37] Chang, Y. M., and Wu, T. L. “On average run lengths of control charts for autocorrelated processes.” *Methodology and Computing in Applied Probability*, 13(2), pp. 419-431 (2011).

[38] Hamdi-Asl, A., Amoozad-Khalili, H., Tavakkoli-Moghaddam, R., et al., “Toward sustainability in designing agricultural supply chain network: A case study on palm date.” *Scientia Iranica.* (2021).

[39] Fasihi, M., Tavakkoli-Moghaddam, R., Najafi, S. E., et al., “Optimizing a bi-objective multi-period fish closed-loop supply chain network design by three multi-objective meta-heuristic algorithms.” *Scientia Iranica.* (2021).

[40] Abbaszadeh, N., Asadi-Gangraj, E., and Emami, S. "Flexible flow shop scheduling problem to minimize makespan with renewable resources." *Scientia Iranica*, 28(3), pp. 1853-1870 (2021).

[41] Stoykova, S., and Spasov, V. "Choice of fitness functions and parameter settings in Genetic Algorithms for analysis of induction motors." In IOP Conference Series: Materials Science and Engineering (Vol. 618, No. 1, p. 012024). IOP Publishing. (2019)

[42] Stoykova, S., and Spasov, V. "Determining the parameters of induction motors by Genetic Algorithms." In IOP Conference Series: Materials Science and Engineering (Vol. 618, No. 1, p. 012023). IOP Publishing. (2019)

[43] Jaiswal, S. and Kumar, N. "Performance Criteria for Evaluation of Control Chart for Phase II Monitoring" *Pramana Research Journal*. 9(2), pp. 406-416 (2019).

[44] Qiao, Y., Hu, X., Sun, J., et al., "Optimal design of one-sided exponential EWMA charts with estimated parameters based on the median run length." *IEEE Access*, 7, pp. 76645-76658 (2019).

Biographies:

Maryam Askari is a Ph.D. student of Industrial Engineering at K.N. Toosi University of Technology. She received her MS in Industrial Engineering from Kharazmi University in Tehran, Iran 2020. Her research interests include signal processing, statistical analysis and machine learning.

Orod Ahmadi is an Assistant Professor of Industrial Engineering at Kharazmi University. He received his Ph.D. in Industrial Engineering from K.N. Toosi University of Technology in Tehran, Iran 2015. His research interests include statistical quality control, time series analysis, applied multivariate statistics, robust statistics, artificial intelligence, machine learning, and data analysis.

Youness Javid is an Assistant Professor at the University of Kharazmi, Tehran, Iran. His research interests include quality engineering, reliability, machine learning, and risk

management. He received his BS from Tabriz University and his MS and Ph.D. degrees from K.N. Toosi University of Technology.

Figure Captions

Figure 1: Block diagram of a linear system
Figure 2: The co-occurrence network of essential keywords
Figure 3: Modulus of frequency response for an ideal lowpass filter
Figure 4: Location of poles for a stable lowpass filter
Figure 5: Mean values of SN ratio for different levels of GA parameters
Figure 6: Zeros and poles of the optimal second-order filter for $\gamma = 0.5$
Figure 7: Modulus of the frequency response of the optimal second-order filter
Figure 8: ARL comparison for the first scenario
Figure 9: MRL comparison for the first scenario
Figure 10: ARL comparison for the second scenario
Figure 11: MRL comparison for the second scenario
Figure 12: ARL comparison for the third scenario
Figure 13: MRL comparison for the third scenario
Figure 14: PFS for the first scenario
Figure 15: PFS for the second scenario
Figure 16: PFS for the third scenario
Figure 17: Time series plot of OPEC basket oil price
Figure 18: Sample ACF and sample PACF of OPEC basket oil price
Figure 19: Sample ACF and sample PACF of the first 150 differenced observations
Figure 20: Control charts of residuals

Table Captions

Table 1: Summarized literature review
Table 2: Description of model parameters and decision variables
Table 3: Levels of GA parameter used in the Taguchi design
Table 4: Parameters of the optimal second-order filter and the corresponding control chart
Table 5: Test statistics and control limits of the Shewhart and the EMWA control charts

Figures:

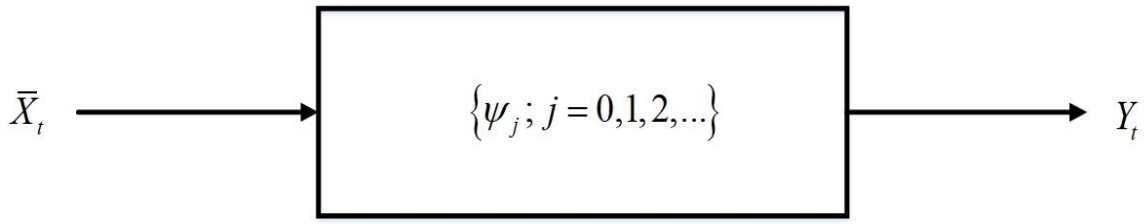

Figure 1: Block diagram of a linear system

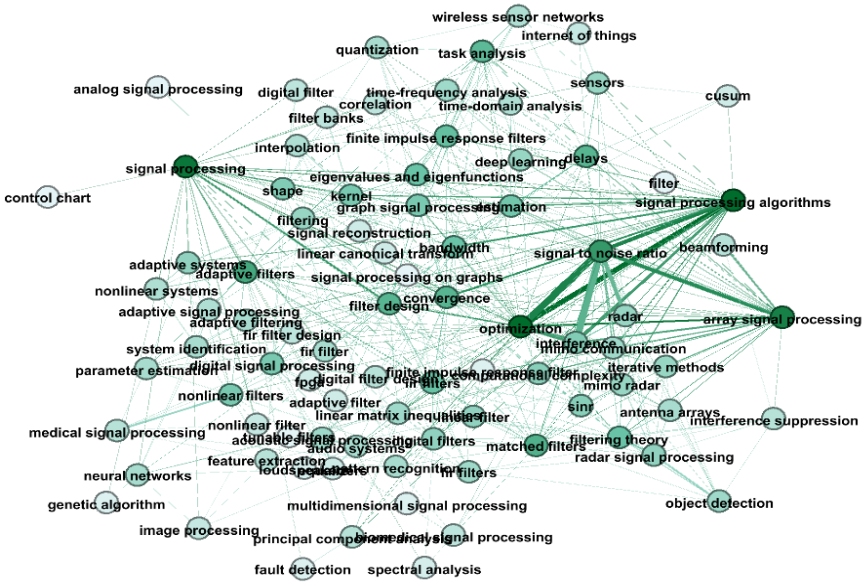

Figure 2: The co-occurrence network of essential keywords

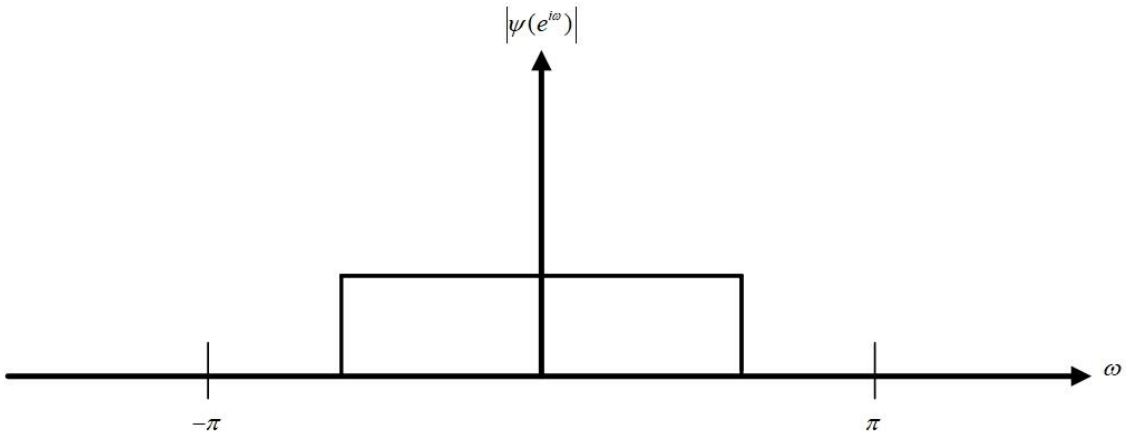

Figure 3: Modulus of frequency response for an ideal lowpass filter

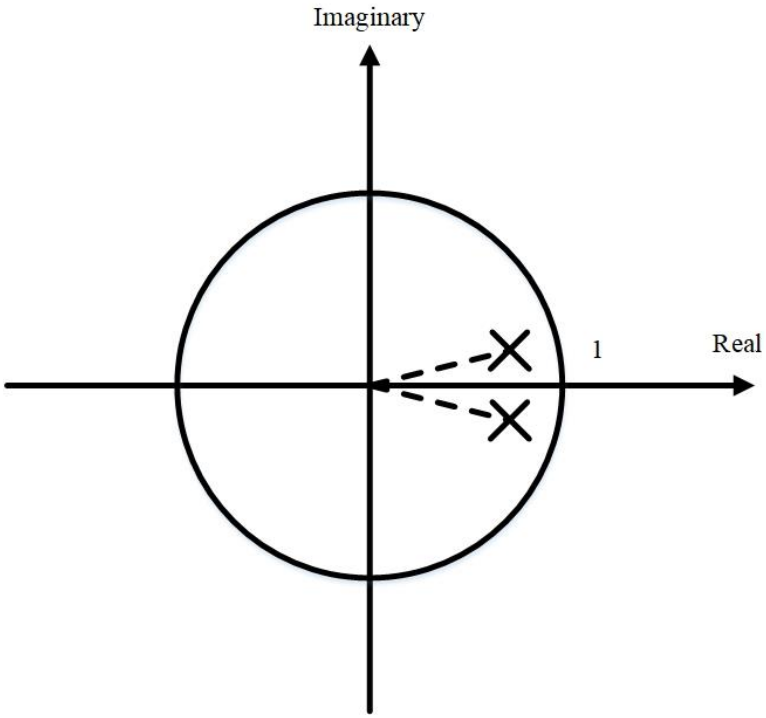

Figure 4: Location of poles for a stable lowpass filter

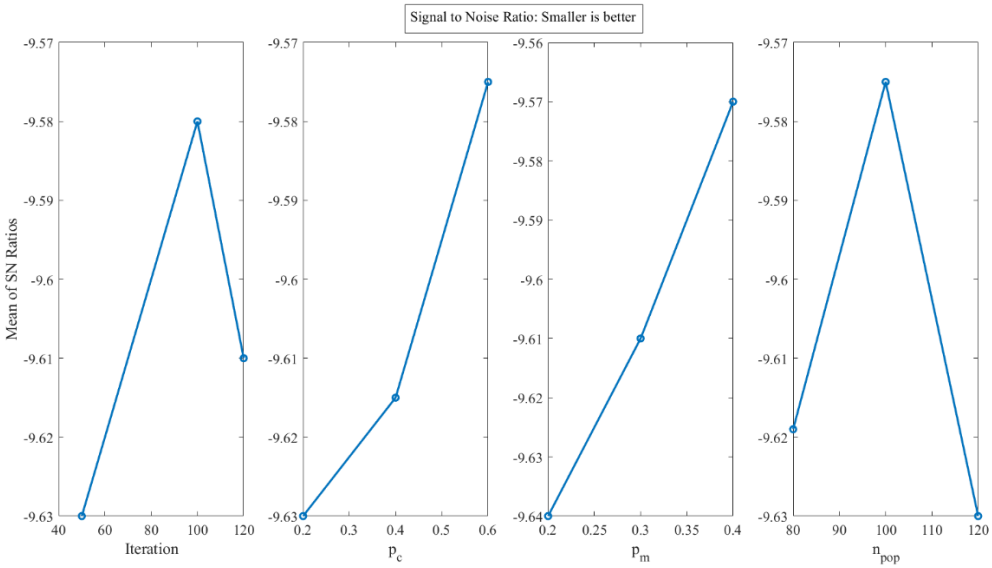

Figure 5: Mean values of SN ratio for different levels of GA parameters

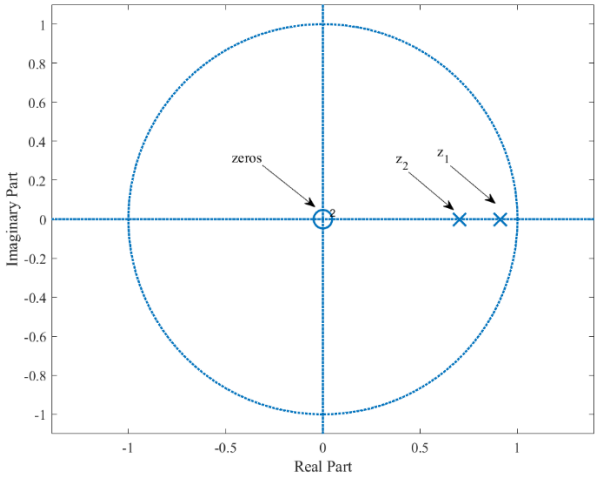

Figure 6: Zeros and poles of the optimal second-order filter for $\gamma = 0.5$

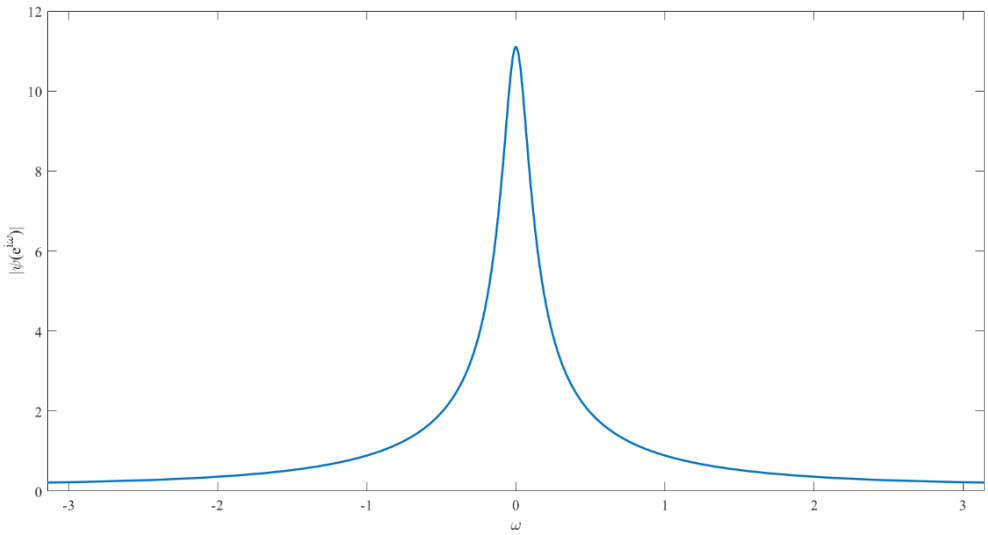

Figure 7: Modulus of the frequency response of the optimal second-order filter

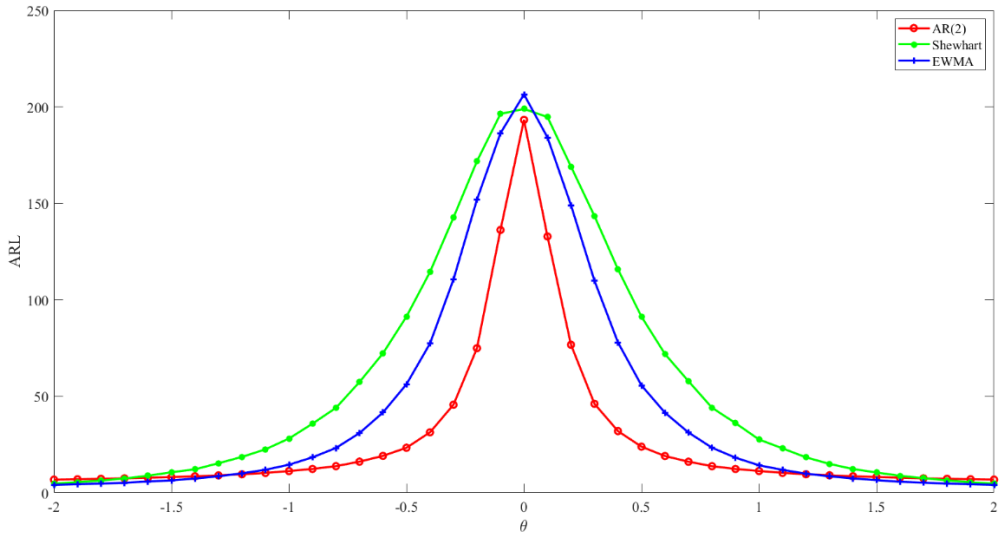

Figure 8: ARL comparison for the first scenario

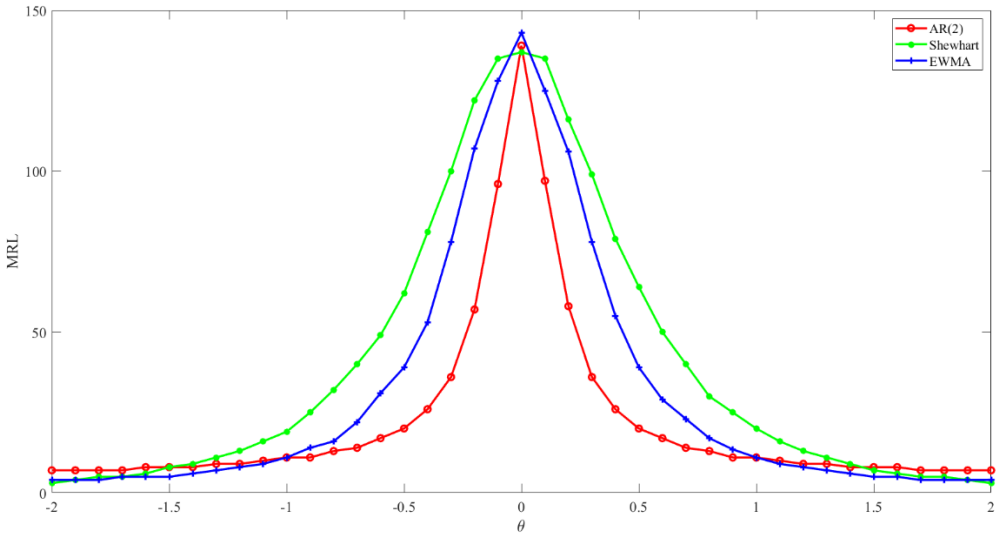

Figure 9: MRL comparison for the first scenario

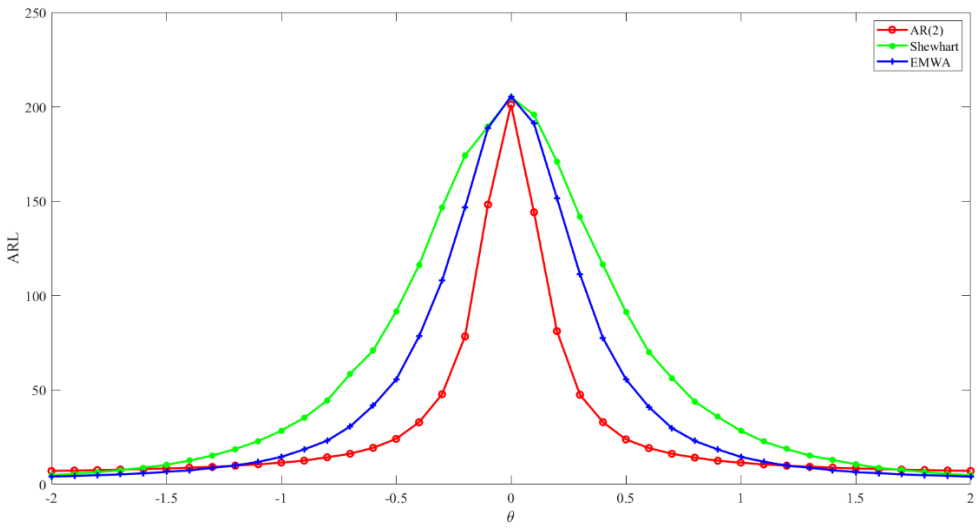

Figure 10: ARL comparison for the second scenario

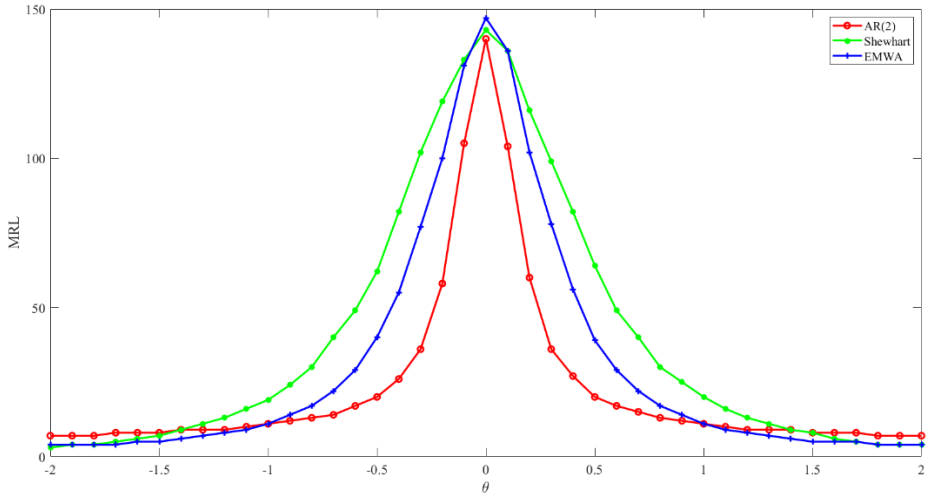

Figure 11: MRL comparison for the second scenario

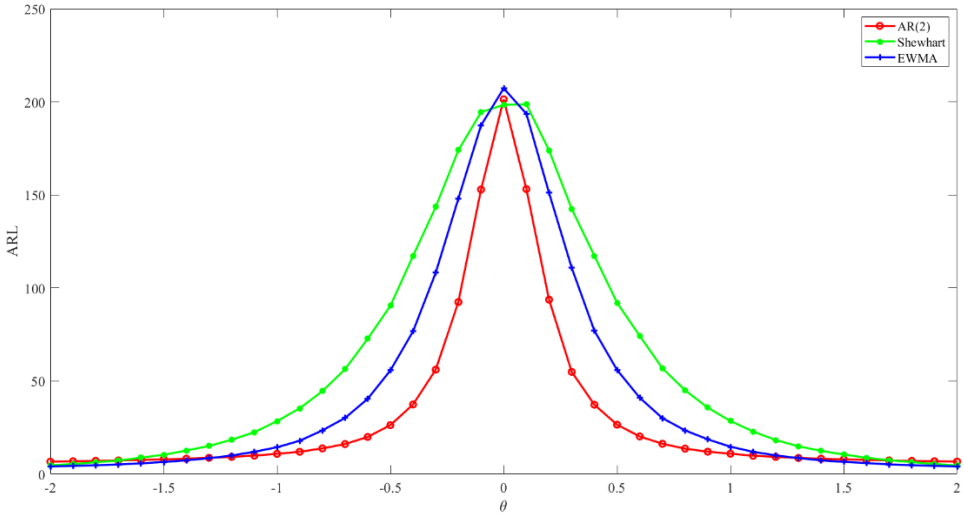

Figure 12: ARL comparison for the third scenario

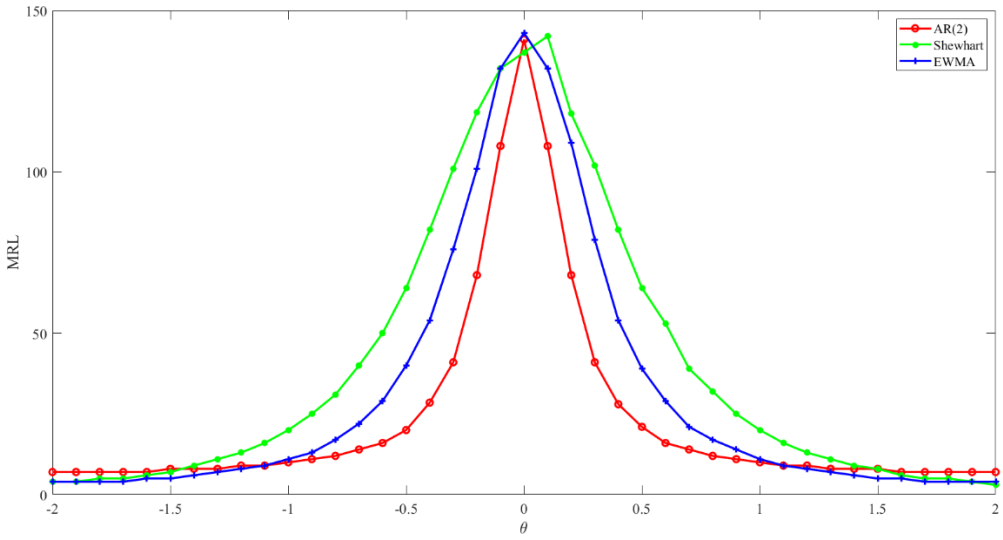

Figure 13: MRL comparison for the third scenario

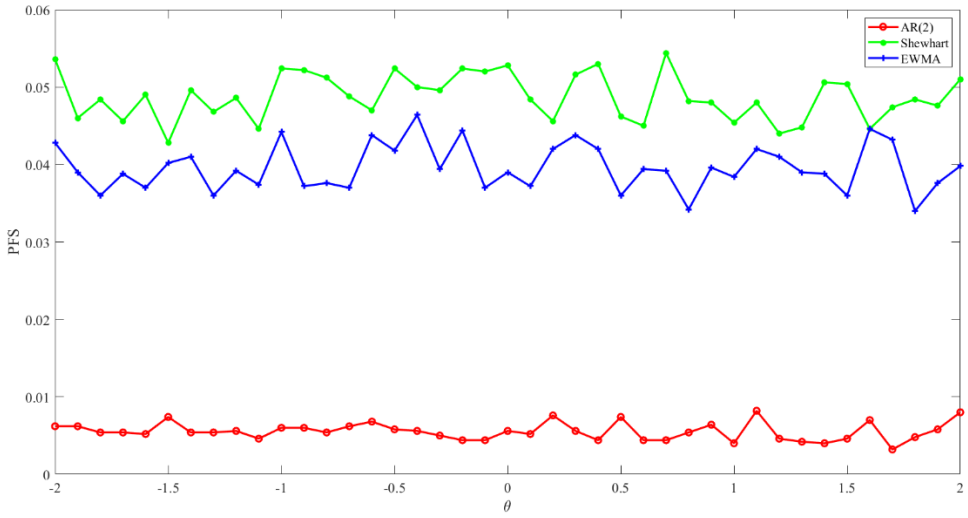

Figure 14: PFS for the first scenario

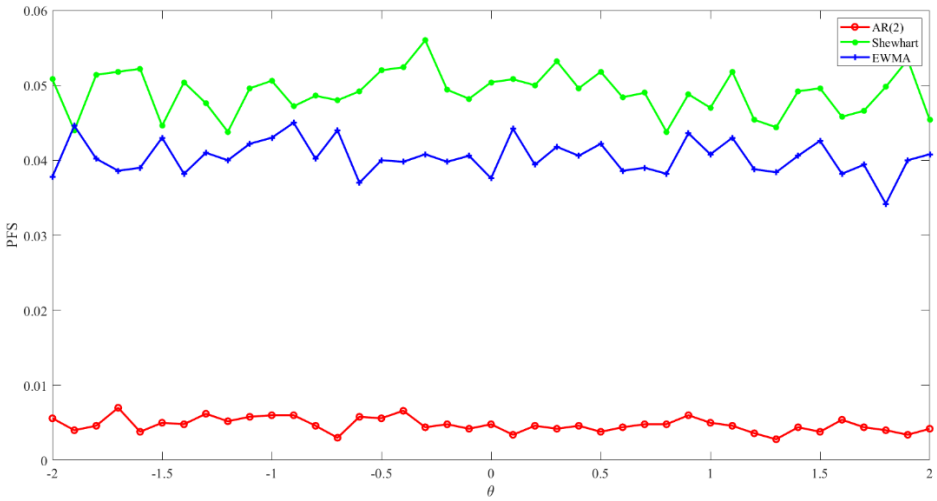

Figure 15: PFS for the second scenario

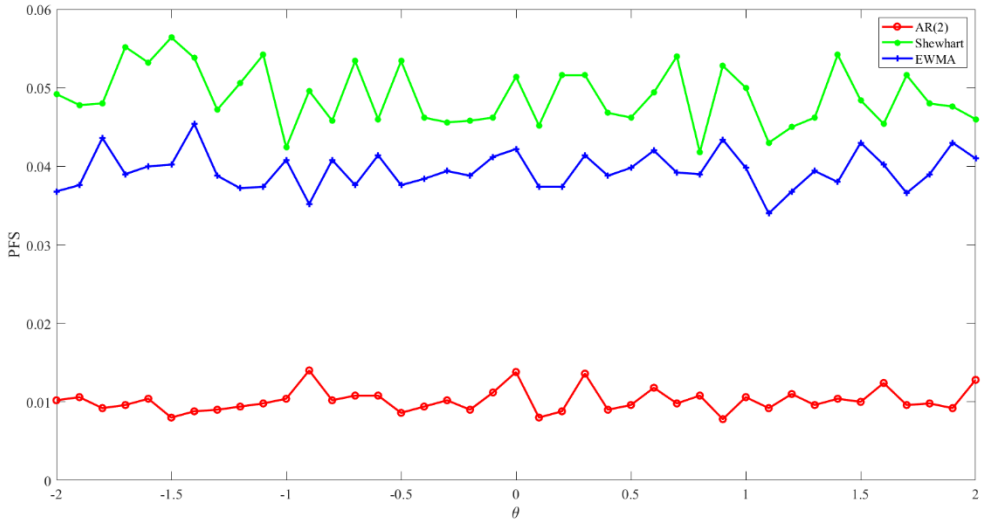

Figure 16: PFS for the third scenario

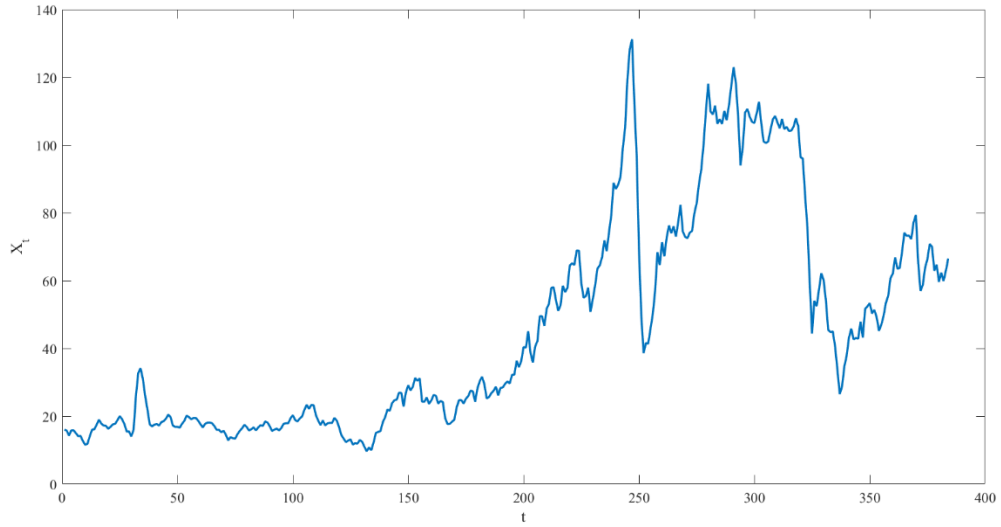

Figure 17: Time series plot of OPEC basket oil price

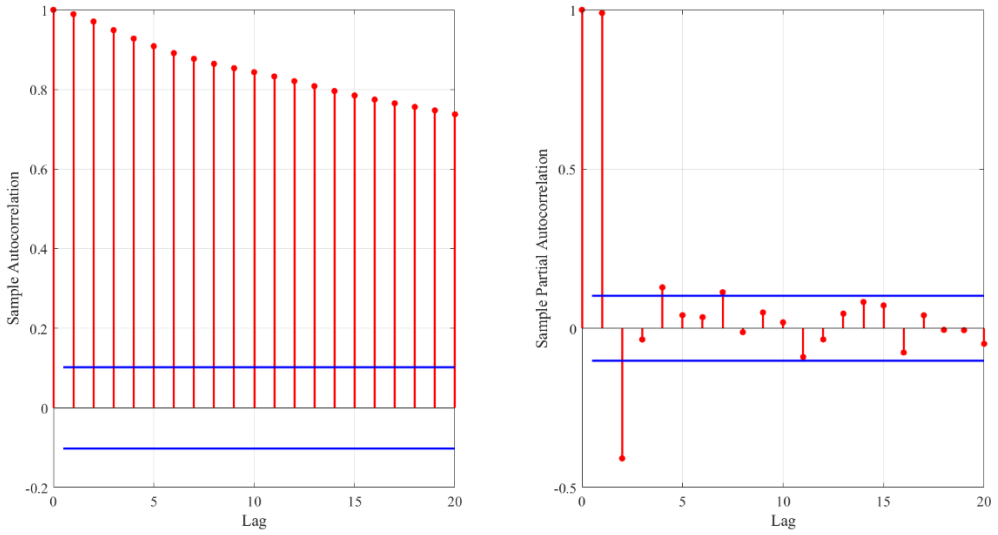

Figure 18: Sample ACF and sample PACF of OPEC basket oil price

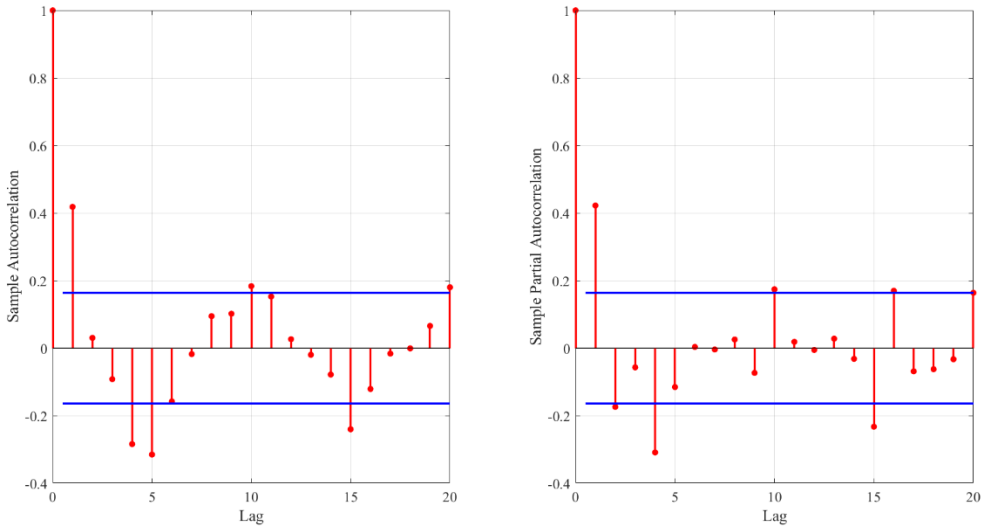

Figure 19: Sample ACF and sample PACF of the first 150 differenced observations

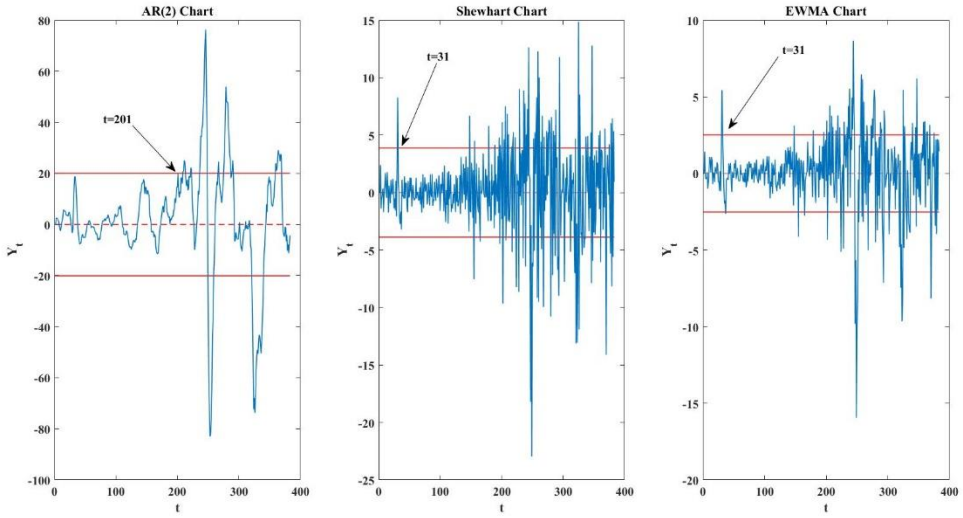

Figure 20: Control charts of residuals

Tables:

Table 1: Summarized literature review

		Domain		Optimization	
Designing approach		Time	Frequency	Time	Time and frequency
ARMA control chart		*	-	*	-
EWMA control chart		*	-	*	-
CUSUM control chart		*	-	*	-
Control chart for autocorrelated observation		*	-	*	-
Filtering	General filter	*	-	*	-
	Second-order filter	*	*	-	-

Table 2: Description of model parameters and decision variables

Symbol	Type	Description
n	Parameter	Sample size
μ_0	Parameter	In-control process mean
σ_0	Parameter	In-control process standard deviation
γ	Parameter	Critical shift
ϕ_1	Continuous Decision Variable	Coefficient of the proposed filter
ϕ_2	Continuous Decision Variable	Coefficient of the proposed filter
L	Continuous Decision Variable	Coefficient of the proposed control chart

Table 3: Levels of GA parameter used in the Taguchi design

Parameter	Level I	Level II	Level III
P_c	0.2	0.4	0.6
P_m	0.2	0.3	0.4
n_{pop}	80	100	120
iteration	50	100	120

Table 4: Parameters of the optimal second-order filter and the corresponding control chart

Critical Shift		ϕ_1	ϕ_2	L
γ	0.25	1.5055	-0.5356	2.1323
	0.5	1.6111	-0.6380	2.1478
	1	1.6644	-0.7066	2.2732

Table 5: Test statistics and control limits of the Shewhart and the EMWA control charts

Control chart	Test Statistics (Y_t)	LCL	UCL
Shewhart	$\bar{X}_t$	$\mu_0 - L\frac{\sigma_0}{\sqrt{n}}$	$\mu_0 + L\frac{\sigma_0}{\sqrt{n}}$
EWMA	$(1-\lambda)Y_{t-1} + \lambda\bar{X}_t$	$\mu_0 - L\sigma_0\sqrt{\frac{\lambda}{(2-\lambda)n}}$	$\mu_0 + L\sigma_0\sqrt{\frac{\lambda}{(2-\lambda)n}}$